Quantum Sieving in Carbon Nanotubes and Zeolites

Qinyu Wang,[1] Sivakumar R. Challa,[1] David S. Sholl,[2] and J. Karl Johnson[1,*]

[1]*Department of Chemical and Petroleum Engineering, University of Pittsburgh, Pittsburgh, Pennsylvania 15261*

[2]*Department of Chemical Engineering, Carnegie Mellon University, Pittsburgh, Pennsylvania 15213*

(Received 30 September 1998)

Fluids adsorbed in microporous materials can exhibit quantum sieving, where heavy isotopes are preferentially adsorbed over light isotopes. We present the first detailed predictions of quantum sieving based on realistic models of microporous materials. Carbon nanotubes, and the interstices of nanotube bundles, can act as highly effective quantum sieves for hydrogen isotopes. Quantum sieving of He and Ne in the zeolite $AlPO_4$-22 is also discussed. [S0031-9007(98)08350-1]

PACS numbers: 64.75.+g, 05.30.–d, 67.70.+n, 82.60.Lf

Molecular sieves are microporous materials that can allow separation of mixtures based on molecular size and shape [1]. Despite wide applications in separations and catalysis, molecular sieving has not been used to separate isotopes because, classically speaking, different isotopes have the same size. Separation of isotopic mixtures is a difficult and energy intensive process requiring special techniques such as chemical exchange, diffusion separation, biological separation, and laser isotope separation [2–4]. In this paper we demonstrate that mixtures of light isotopes can be selectively adsorbed in very small pores, leading to a novel separation technique called quantum sieving. Molecular sieving excludes molecules that are physically larger than the pores of the adsorbent, resulting in selective adsorption of smaller molecules. Quantum sieving excludes lighter molecules from pores in favor of heavier molecules because the higher zero-point energy of the light species makes their adsorption energetically unfavorable. Quantum sieving was first proposed by Beenakker *et al.* [5], based on a simple model of adsorption of hard spheres in hard cylindrical pores. In this paper we present the first assessment of this effect using realistic descriptions of molecules and microporous adsorbents. A simple theoretical model and extensive path integral calculations both indicate that molecular tritium will readily adsorb in appropriately sized micropores that exclude molecular hydrogen through quantum sieving. Interstitial channels of close-packed carbon nanotube bundles or ropes have the correct pore size and solid-fluid potential to effectively sieve mixtures of H_2 and T_2. Quantum sieving can also be observed using opened single-walled carbon nanotubes, but the effect is significant only for nanotubes with diameters smaller than any observed experimentally.

Our theoretical treatment begins by considering a low-pressure binary gas mixture in equilibrium with an adsorbed phase. We assume that at a sufficiently low density the adsorbate forms a classical 1D gas, with unhindered axial translational motion, and that the transverse (radial) degrees of freedom are quantized and in their ground state. The ground state energy of species i's transverse wave function is denoted by E_i. The chemical potential of this adsorbed species is [6,7]

$$\mu_i = E_i + k_B T \ln\left(\frac{\rho_i \lambda_i}{q_i^{\text{int}}}\right), \tag{1}$$

where ρ_i is the number density of component i in the pore, λ_i is the de Broglie thermal wavelength, q_i^{int} is the internal partition function, k_B is the Boltzmann constant, and T is the absolute temperature. The chemical potential of the bulk gas, considered to be ideal, is

$$\mu_i^{\text{bulk}} = k_B T \ln\left(\frac{n_i \lambda_i^3}{q_i^{\text{int}}}\right), \tag{2}$$

where n_i is the gas phase density of component i. At equilibrium, $\mu_i = \mu_i^{\text{bulk}}$, so the adsorbate density is [6,7]

$$\rho_i = n_i \lambda_i^2 e^{-E_i/k_B T}. \tag{3}$$

We define the selectivity of component 1 to 2 by $S = (x_1/x_2)/(y_1/y_2)$, with x_i (y_i) the pore (bulk) mole fractions, and denote the selectivity in the limit of zero pressure by S_0. This gives

$$S_0 = \frac{(\rho_1/\rho_2)}{(n_1/n_2)} = \frac{m_2}{m_1} \exp\left[-\frac{E_1 - E_2}{k_B T}\right], \tag{4}$$

where m_i is the molecular mass of component i. We should note that corresponding expression for the selectivity of hard spheres in hard cylinders as given by Beenakker *et al.* [5] is erroneously missing the ratio of the masses. If, for example, the adsorbate-pore potential is well approximated by a radially symmetric harmonic potential, $V(r) = kr^2/2$, the ground state energies for isotopes of mass m_1 and m_2 are $E_i = \hbar\sqrt{k/m_i}$, and the zero pressure selectivity is given by

$$S_0 = \frac{m_2}{m_1} \exp\left[-\frac{\hbar\sqrt{k}}{k_B T}\left(\frac{1}{\sqrt{m_1}} - \frac{1}{\sqrt{m_2}}\right)\right]. \tag{5}$$

In the case of isotope mixtures, both the species are subject to the same adsorption potential, so the preferential adsorption of the heavier isotope is due purely to quantum confinement.

Adsorption potentials can often be represented accurately with atom-atom potential functions, such as the

 0031-9007/99/82(5)/956(4)$15.00

Lennard-Jones potential [8]. We have taken this approach in constructing realistic solid-fluid potentials. To evaluate S_0 using Eq. (4), the ground state energies of realistic potentials can be computed by expanding the wave functions with a 2D harmonic oscillator basis set and computing the eigenvalues of the resulting Hamiltonian matrix [9]. Alternatively, S_0 can be calculated directly using a path integral formalism [10],

$$S_0 = \frac{\int d\Gamma_1 \int d\omega_1 \int_0^R dr\, r \exp[-U_1/k_B T]}{\int d\Gamma_2 \int d\omega_2 \int_0^R dr\, r \exp[-U_2/k_B T]}, \quad (6)$$

where U is the configurational energy, Γ and ω are the path's internal conformation and orientation, respectively, r is the radial position of the ring's center of mass, and R is the tube's radius. Angular and radial integrations were performed numerically. Integrations over Γ were performed by drawing random ring conformations from the ideal gas distribution [11].

Effective quantum sieving requires sorbents with pore widths slightly larger than the molecular diameters of the adsorbate molecules. Fullerene single-wall carbon nanotubes (SWNTs) are excellent candidates for quantum sieving sorbents. SWNTs self-organize into crystalline ropes comprised of hundreds of SWNTs in a 2D triangular lattice [12]. As produced, SWNTs are capped at their ends; procedures have been devised to remove end caps without destroying the nanotubes [13–15]. Tubes can also be purified and processed into short, open-ended pipes [15]. Once the caps have been removed, the tubes can be used for gas adsorption. For example, hydrogen can be adsorbed into opened SWNTs with diameters of about 12 Å [13]. The 12 Å tube is the same diameter as the (9,9) tube, in the notation of Hamada *et al.* [16]. Using the methods described above, we have computed zero-pressure selectivities for SWNTs of various diameters. Figure 1 is a plot of S_0 at a temperature of 20 K for a mixture of H_2 and T_2 as a function of tube diameter, d. The solid-fluid potential was generated for various (n, m) tubes by using the Crowell-Brown potential [17] for hydrogen-carbon interactions and performing axial and angular averaging to produce a smoothed 1D potential for each tube. Isosteric heats of adsorption and adsorption isotherms for hydrogen on graphite computed from the Crowell-Brown potential are in good agreement with experimental data [18,19]. The agreement between Eq. (4) and the path integral simulations is excellent. The family of possible SWNTs includes only a discrete set of pore diameters, so the data in Fig. 1 do not form a continuous curve. Moreover, helicity effects mean that two tubes with almost identical d can have values of S_0 that differ appreciably from a smooth curve fitted through the data in Fig. 1. Despite these subtleties, Fig. 1 shows that SWNTs wider than $d \simeq 7$ Å exhibit weak selectivity due to quantum sieving while smaller SWNTs are predicted to exhibit very large selectivities.

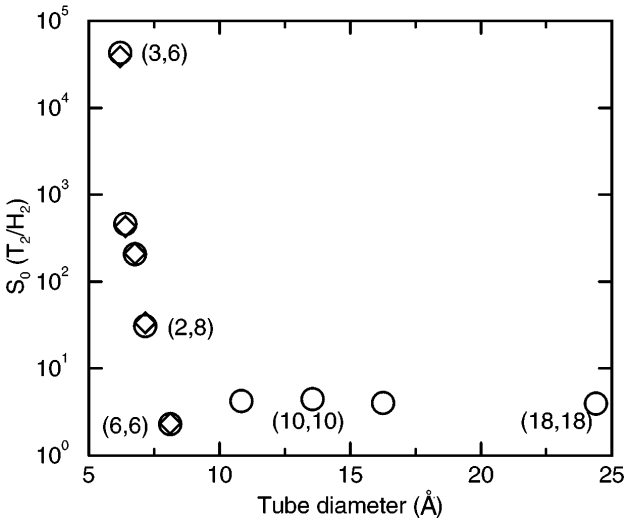

FIG. 1. S_0 at 20 K for T_2/H_2 as a function of tube radius. Results from Eq. (4) (diamonds) and path integral calculations (circles) are shown. A few specific tubes are labeled on the graph with their (n, m) indices.

Equation (4) is only valid at extremely low temperatures and pressures. To explore the possibility of isotopic separations at arbitrary pressures and finite temperatures, we have used path integral grand canonical Monte Carlo (PI-GCMC) simulations to compute the pure component isotherms of hydrogen isotopes in SWNTs. This method correctly accounts for finite temperature effects and fluid-fluid interactions. Details of the PI-GCMC method have been presented previously [11,18,20]. PI-GCMC isotherms for adsorption of pure T_2 and H_2 in the (3,6) nanotube (diameter 6.2 Å) are shown in Fig. 2. The temperature is 20 K and the pressure ranges from 10^{-14} to 100 torr. Recall that the solid-fluid potential for H_2 is exactly the same as for T_2 in these calculations, so the difference between the adsorption isotherms is solely due to quantum effects. There is a very wide pressure range that corresponds to T_2 adsorbing in the (3,6) tube while H_2 is effectively excluded. However, these pressures are extremely small, corresponding to ultrahigh vacuum conditions.

Unfortunately, the diameters that are effective for quantum sieving in SWNTs correspond to tubes which, although theoretically feasible, have not yet been made. The smallest nanotubes produced so far have diameters of approximately 7 Å [21]. However, bundles of SWNTs have interstitial channels that are smaller in diameter than the tubes. Stan *et al.* have performed theoretical calculations showing that He and Ne can be strongly physisorbed inside these interstices [7]. Interstitial diameters are proportional to the diameter of the tubes which make up the bundle. The interstitial regions of the (10,10) tube are precisely the correct size for quantum sieving of mixtures of H_2 and T_2. The (10,10) tube has a diameter of 13.6 Å, very close to the diameter of tubes that can be

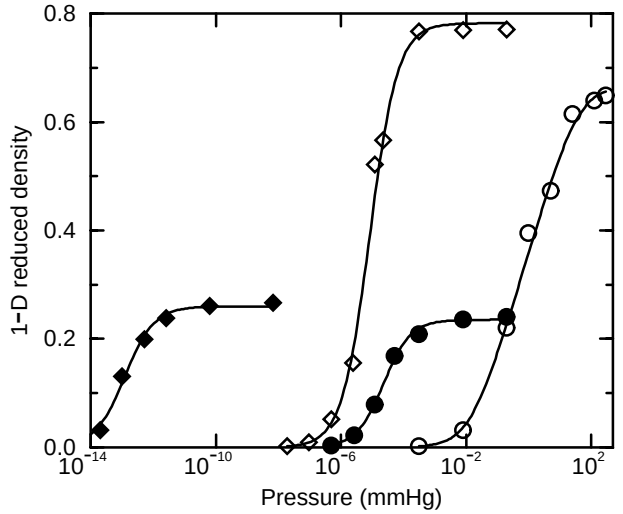

FIG. 2. Adsorption isotherms for T_2 (diamonds) and H_2 (circles) adsorbed inside a (3,6) nanotube (filled symbols) and the interstices of a (10,10) tube (open symbols) at 20 K from PI-GCMC. The density is reduced with respect to the fluid-fluid interaction potential diameter. The lines are fits to the data with the Langmuir uniform distribution isotherm model [23].

produced in high concentrations [12]. Pure fluid adsorption isotherms for H_2 and T_2 in (10,10) interstices (calculated using PI-GCMC) are plotted in Fig. 2. The potential for the interstice is not cylindrically symmetric. Details of the potential generation have been given previously [20]. The pressure range leading to exclusion of H_2 but not T_2 in the interstitial region is smaller than for the (3,6) SWNT, but the pressures are much more accessible experimentally. It appears that quantum sieving can be observed for this system over several orders of magnitude of pressure.

Pure fluid adsorption isotherms may be used to predict mixture selectivities within the framework of ideal adsorbed solution theory (IAST) [22]. We have used the adsorption data for the (10,10) interstices in Fig. 2 in conjunction with IAST to compute selectivities, S, at two different bulk mole fractions. To apply IAST, we have fitted the pure fluid isotherm for each species with the Langmuir uniform distribution isotherm model [23].

Predictions from IAST are shown in Fig. 3. Note that, in contrast to S, S_0 is independent of the bulk gas composition. At low pressures S computed from IAST converges to a value close to S_0 computed from Eq. (4). Figure 3 provides strong evidence that (10,10) SWNT interstitial pores should exhibit dramatic isotopic separations due to quantum sieving over a large range of pressure and bulk composition. This system provides an excellent target for experimental study of this phenomenon. The large selectivities seen in Fig. 3 also mean that direct PI-GCMC simulations for this system may be subject to large errors due to extremely low mole fractions of adsorbed H_2.

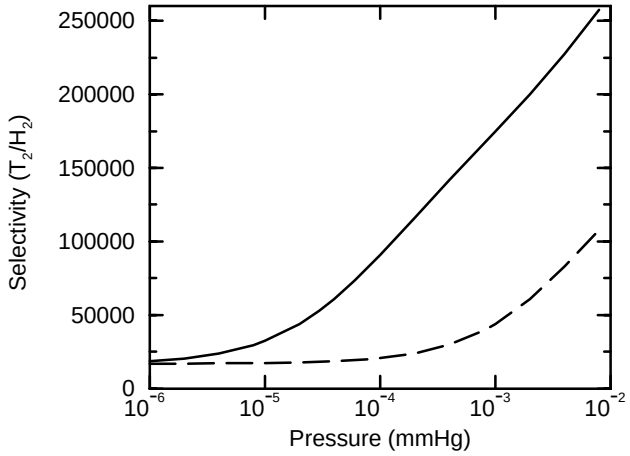

FIG. 3. Selectivity of T_2 to H_2 as a function of pressure for adsorption in the interstitial regions of a (10,10) SWNT bundle at 20 K. The solid (dashed) line corresponds to a bulk gas of 50 (99) mole % H_2.

Quantum sieving is possible not only for isotopic mixtures, but also for mixtures of species with similar (classical) sizes but different masses [5]. Examining a number of zeolites from the standpoint of channel size [24] suggests that the aluminophosphate zeolite $AlPO_4$-22 should have pore sizes roughly in the range required to show quantum sieving for mixtures of He and Ne. $AlPO_4$-22 has unidimensional channels that alternate between cages wide enough for He and Ne molecules to pass one another and narrower necks connecting the cages. We computed the solid-fluid adsorption potentials using a Kiselev-type potential [25] and the experimentally determined crystal structure [26]. Ground state energies for isolated He and Ne inside $AlPO_4$-22 are compared to their classical values as a function of position inside the pore in Fig. 4, allowing

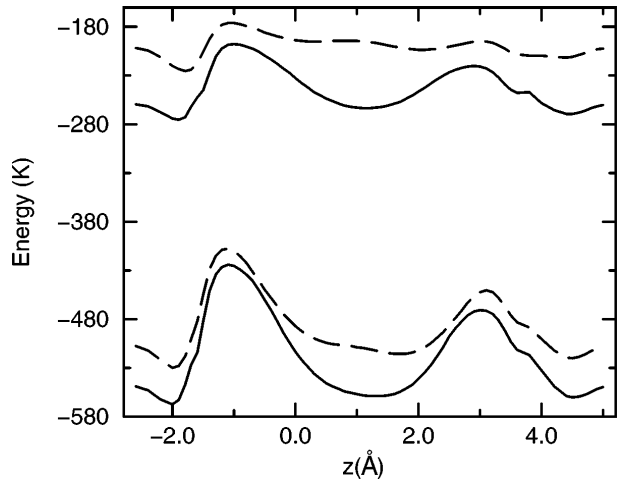

FIG. 4. Ground state energies for He and Ne in $AlPO_4$-22 from classical calculations (solid lines) and the harmonic basis set expansion (dashed lines). The top (bottom) pair of curves is for He (Ne). Slightly more than one unit cell is shown.

several conclusions to be drawn. First, the classical potentials show that Ne is adsorbed much more strongly than He, due to differences in the fluid-solid potentials. This effect is slightly enhanced when quantum confinement is considered. In other words, $S_0(\mathrm{Ne}/\mathrm{He}) \gg 1$, but the majority of this selectivity comes from classical contributions. For both species, the diffusion activation energy is reduced by including zero-point contributions. The Ne activation energy is substantially larger than for He, a fact that could be exploited to achieve selective adsorption of He at low temperatures based on kinetic limitations. Finally, Fig. 4 shows that zero-point effects are important not only in the narrow regions of the pore (approximately $0 < z < 2$ Å, nominal diameter 3.9 Å [24]), but also in the wider cage regions. This effect occurs because in the cages the solid-fluid potential confines molecules to an annular region that exhibits quantum confinement in the radial direction. This effect also appears in SWNTs, as can be seen in Fig. 1, where $S_0 > 1$ for very wide nanotubes. The minimum in S_0 observed in Fig. 1 corresponds to the largest diameter tube giving a single minimum in the potential well. Tubes with larger diameters have an annular minimum near the tube walls and a local maximum in the center of the tube, causing the fluid particles to be quantally confined to the annulus.

We thank George Stan and Milton Cole for helpful discussions. J.K.J. acknowledges the National Science Foundation and Sandia National Laboratory for support of this work.

*Author to whom correspondence should be addressed. Email: karlj+@pitt.edu

[1] R. Szostak, *Molecular Sieves Principles of Synthesis and Identification* (van Nostrand Reinhold, New York, 1989).
[2] *Separation of Isotopes*, edited by H. London (George Newnes Ltd., London, 1961).
[3] I. Sh. Averbukh, M. J. J. Vrakking, D. M. Villeneuve, and A. Stolow, Phys. Rev. Lett. **77**, 3518 (1996).
[4] O. Atabek, M. Chrysos, and R. Lefebvre, Phys. Rev. A **49**, R8 (1994).
[5] J. J. M. Beenakker, V. D. Borman, and S. Yu. Krylov, Chem. Phys. Lett. **232**, 379 (1995).
[6] G. Stan and M. W. Cole, Surf. Sci. **395**, 280 (1998).
[7] G. Stan, V. H. Crespi, M. W. Cole, and M. Boninsegni, J. Low Temp. Phys. **113**, 447 (1998).
[8] G. Vidali, G. Ihm, H-Y. Kim, and M. W. Cole, Surf. Sci. Rep. **12**, 133 (1991); W. Steele, Chem. Rev. **93**, 2355 (1993).
[9] S. Hammes-Schiffer and J. C. Tully, J. Chem. Phys. **101**, 4657 (1994).
[10] R. P. Feynman, Rev. Mod. Phys. **20**, 367 (1948); R. P. Feynman and A. R. Hibbs, *Quantum Mechanics and Path Integrals* (McGraw-Hill, New York, 1965).
[11] Q. Wang, J. K. Johnson, and J. Q. Broughton, J. Chem. Phys. **107**, 5108 (1997)
[12] A. Thess *et al.*, Science **273**, 483 (1996).
[13] A. C. Dillon *et al.*, Nature (London) **386**, 377 (1997).
[14] J. Sloan, J. Hammer, M. Zwiefka-Sibley, and M. L. H. Green, Chem. Commun. **1998**, 347 (1998).
[15] J. Liu *et al.*, Science **280**, 1253 (1998).
[16] N. Hamada, S. Sawada, and A. Oshiyama, Phys. Rev. Lett. **68**, 1579 (1992).
[17] A. D. Crowell and J. S. Brown, Surf. Sci. **123**, 296 (1982).
[18] Q. Wang and J. K. Johnson, Mol. Phys. **95**, 299 (1998).
[19] Q. Wang and J. K. Johnson (unpublished).
[20] Q. Wang and J. K. Johnson, J. Chem. Phys. **110**, 577 (1999).
[21] S. Iijima and T. Ichihasi, Nature (London) **363**, 603 (1993).
[22] A. L. Myers and J. M. Prausnitz, AIChE J. **11**, 121 (1965)
[23] R. F. Cracknell and D. Nicholson, J. Chem. Soc. Faraday Trans. **90**, 1487 (1994); R. F. Cracknell and D. Nicholson, Adsorption **1**, 7 (1995).
[24] W. H. Meier and D. H. Olson, *Atlas of Zeolite Structure Types* (Butterworths, London, 1987).
[25] D. S. Sholl and K. A. Fichthorn, J. Chem. Phys. **107**, 4384 (1997).
[26] J. W. Richardson, Jr., J. J. Pluth, and J. V. Smith, Naturewissenschaften **76**, 467 (1989); J. J. Pluth (private communication).